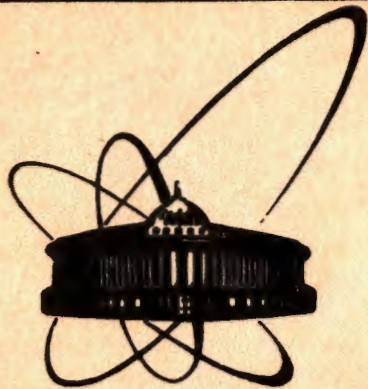


92-283



**ОБЪЕДИНЕННЫЙ
ИНСТИТУТ
ЯДЕРНЫХ
ИССЛЕДОВАНИЙ
ДУБНА**

E15-92-283

**ANTIPROTON-⁴He INTERACTIONS
AT 192.8 MeV/c**

PS 179 COLLABORATION

Submitted to "Physics Letters B"

1992

F.Balestra, S.Bossolasco, M.P.Bussa, L.Bussò, L.Fava, L.Fer-
rero, A.Maggiora, D.Panzieri, G.Piragino, F.Tosello

Instituto di Fisica Generale "A.Avogadro", University of
Torino and INFN - Sezione di Torino, Turin, Italy

Yu.A.Batusov, S.A.Bunyatov, I.V.Falomkin, F.Nichitiu,
G.B.Pontecorvo, A.M.Rozhdestvensky, M.G.Sapozhnikov

Joint Institute for Nuclear Research, Dubna

G.Bendiscioli, V.Filippini, A.Rotondi, P.Salvini, V.I.Tretyak*,
A.Zenoni

Dipartimento di Fisica Nucleare e Teorica, University of
Pavia and INFN - Sezione di Pavia, Pavia, Italy

K.M.Danielsen, T.Jakobsen

Physics Department, University of Oslo, Oslo, Norway

C.Guaraldo

Laboratori Nazionali di Frascati dell'INFN, Frascati, Italy

A.Haatuft, A.Halsteinslid, K.Myklebost, J.M.Olsen

Physics Department, University of Bergen, Bergen, Norway

E.Lodi Rizzini

Dipartimento di Automazione Industriale, University of
Brescia, Brescia and INFN - Sezione di Pavia, Pavia, Italy

*On leave

The experimental data on antiproton interaction with light nuclei provides valuable information for understanding of antiproton-nucleus dynamics, for example, for determining the parameters of the antiproton-nucleus potential. Since a reliable description of the elastic scattering is a necessary condition for any adequate model of $\bar{p}A$ -scattering, any new information on the differential elastic scattering cross sections serves as a test for the various models of $\bar{p}A$ -interaction. Besides this, the data on elastic scattering on the lightest nuclei can be used for determining the parameters of the elementary amplitude of antiproton interaction with neutrons which, owing to the absence of good antineutron beams, are not well known.

At present data are available on the elastic scattering of antiprotons on deuterium [1,2], on ^{12}C , ^{40}Ca and ^{208}Pb at 300 and 600 MeV/c [3,4], and on ^{16}O and ^{18}O at 600 MeV/c [5] and on ^4He [6] as well. The last result was obtained by our group in the PS-179 (CERN) experiment.

We have observed that at 600 MeV/c the $\bar{p}^4\text{He}$ elastic scattering exhibits a diffraction pattern typical of scattering on a strongly absorbing disk. The fuzzy-black-disk model [7] and Glauber model calculations were found to provide a good agreement with the experimental data.

Here we present the results of the PS-179 (CERN) experiment on the investigation of $\bar{p}^4\text{He}$ interaction at 192.8 MeV/c ($T_{\text{kin}}=19.6$ MeV). At this energy $\bar{p}^4\text{He}$ interaction includes only elastic scattering and annihilation, being below the threshold for charge-exchange (\bar{p}, \bar{n}) and ^4He break-up (\bar{p}, \bar{p}') reactions.

Measurements were performed in the LEAR antiproton beam at CERN using a streamer chamber placed in a magnetic field. The experimental setup is shown in Fig.1. The apparatus was triggered by coincidence signals from the counters C_2 and C_4 and anticoincidence signals from the counters of the "live" collimator C_1 and C_3 and from the counter C_5 situated after the chamber. Therefore, a trigger occurred, when an antiproton entered the chamber, but did not hit counter C_5 at the exit window.

The (90x70x18) cm^3 streamer chamber, operated in self-shunting mode [8], was filled with helium at NTP. The chamber was placed in a magnetic field of 0.4 T or 0.6 T.

УСЛОВИЯ ИСПЫТАНИЯ
ИСПЫТАТЕЛЬНАЯ СИСТЕМА
БИБЛИОТЕКА

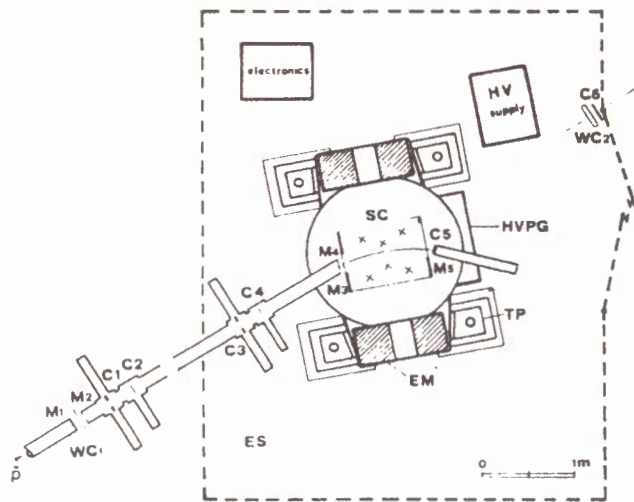


Fig.1. Layout of the experimental apparatus. EM - electromagnet; SC - streamer chamber; HVPG - high voltage pulse generator; TP - travelling platform; ES - electrostatic screening; WC₁₋₂ - wire chambers; C₁₋₆ - scintillation counters; M₁₋₅ - thin walls.

The sensitive volume of the streamer chamber was photographed using two cameras with parallel optical axes 280 mm apart. Each photograph represented a picture of a sole antiproton interaction event with helium. A detailed description of the experimental apparatus can be found elsewhere [9].

Approximately 10^5 pictures with photos of antiproton ${}^4\text{He}$ interactions were processed. We scanned them twice. The zone 54 cm long at the center of the chamber was chosen for multiplicity and cross section measurements.

As a result we have found 2135 events with multiplicity other than 2, which are obviously annihilation events, and 1431 two-prong events, which may be either elastic scattering or annihilation events. The efficiency of scanning is equal to 99%. 1414 of the found two-prong events are measured. The geometrical reconstruction of the measured events was performed with the aid of a program written within the HYDRA system [10]. The input errors used for the HYDRA geometrical reconstruction program were the same as in our previous work [11]. 1237 of these events

passed the geometrical reconstruction. So the measurement and reconstruction procedure efficiency is $\epsilon = 86.4\%$.

Final sample of events comprises of 1053 events with the c.m. scattering angle $\theta > 12^\circ$. For identification of elastic scattering events we compared the characteristics of the secondary particles (momentum, scattering angle, range etc.) for each event with the corresponding quantities calculated assuming elastic scattering kinematics. Criteria involving the following four quantities were used to select elastic scattering events: 1) recoil nucleus angle; 2) coplanarity; 3) recoil nucleus range (if it stopped) or its momentum (if it did not stop); 4) scattered antiproton momentum. 977 events passed all four criteria.

The remaining 76 events are inelastic. Considering the scanning, measurement and reconstruction efficiency, the total number of inelastic two-prong events is 103 and the total number of inelastic events is 2238.

The corresponding antiproton ${}^4\text{He}$ annihilation cross section is obtained equal to

$$\sigma_a = 377.6 \pm 8.0 \text{ mb.}$$

A systematic error was estimated to be less than 2.5% due to uncertainties in the target transparency and the number of incoming antiprotons. Our previous measurements [12,13] of σ_a and of multiplicities involving a lower statistics (600 events) agree within the statistical errors with the present results.

Table 1. Multiplicity distributions (%) in $\bar{p}{}^4\text{He}$ annihilation at different energies [14,15]

M	at rest	192.8 MeV/c	608 MeV/c
1	3.36 ± 0.35	5.94 ± 0.50	5.80 ± 0.43
2	5.03 ± 0.42	4.60 ± 0.44	4.32 ± 0.38
3	33.48 ± 0.92	32.62 ± 0.99	29.53 ± 0.85
4	12.26 ± 0.63	10.81 ± 0.66	8.12 ± 0.51
5	35.68 ± 0.93	36.51 ± 1.01	41.17 ± 0.92
6	3.51 ± 0.36	2.64 ± 0.34	2.99 ± 0.31
7	6.24 ± 0.47	6.40 ± 0.52	8.07 ± 0.51
8	0.19 ± 0.08	0.22 ± 0.10	0.19 ± 0.08
9	0.24 ± 0.10	0.22 ± 0.10	0.12 ± 0.07
$\langle M \rangle$	4.097 ± 0.072	4.025 ± 0.078	4.181 ± 0.074
${}^3\text{He}+X, (\%)$	21.0 ± 0.9	18.3 ± 0.5	15.6 ± 0.7

The charged prong multiplicity distribution is compared with those for annihilation of stopped antiprotons and at 608 MeV/c in Table 1. One can see that the energy dependence of the multiplicity distribution is rather weak.

Especially interesting (for instance, for astrophysics [16,17]) is the reactions with ${}^3\text{He}$ formation in the final state. The signature of these reactions in $\bar{p}{}^4\text{He}$ annihilation is unambiguous: they are the only processes with odd number of prongs in the final state. The branching ratios of the ${}^3\text{He}$ formation at different energies are also given in Table 1. One can see that they decrease with energy owing to increasing the FSI interactions which destroyed ${}^3\text{He}$ nuclei.

It must be stressed that a streamer chamber operating at normal pressure represents a very good instrument for studying charged-particle multiplicities. For instance, the tracks of a 250 keV α -particle or a 160 keV proton are 1 cm long in the chamber and are quite visible.

Antiprotons scattered at small angles could hit the anticoincidence counter C_5 , resulting in the event not being recorded. The loss of events due to scattered antiprotons hitting the anticoincidence counter C_5 was taken into account by introduction of a weight $W_i = 1/\epsilon_{C5}(i)$ for each event of scattering angle θ_i . These weights increased from 0.85 to 1.0, with the scattering angles in lab.sys. changing from 10° to 18° .

Differential cross sections were calculated by the formula

$$\frac{d\sigma}{d\Omega} = \frac{\sum_i W_i}{\sigma_0 \epsilon \cdot \Delta\Omega},$$

where $\sigma_0 = N_{\text{dose}} \cdot \rho \cdot L$, $N_{\text{dose}} \approx 4.5 \cdot 10^6$ is the number of antiprotons that transverse the target, ρ is the number of ${}^4\text{He}$ nuclei per unit volume, L is the mean path length of the antiprotons in the fiducial volume, ϵ is the overall efficiency of scanning, measurement and geometrical reconstruction of events (which varies from $\epsilon=0.73$ at small scattering angles up to $\epsilon=0.93$ at large scattering angles), W_i are the weights of events in the angular interval $\Delta\Omega$. The obtained $d\sigma/d\Omega$ is shown in Table 2.

For determination of the total $\bar{p}{}^4\text{He}$ elastic scattering cross section the differential cross section was approximated by the following expression:

$$d\sigma/d\Omega = |F_{\text{Coul}}(\theta) + F_{\text{nucl}}(\theta)|^2, \quad (1)$$

where the nuclear amplitude $F_{\text{nucl}}(\theta)$ was taken in the form:

$$F_{\text{nucl}}(\theta) = \sigma_{\text{tot}} k(i+\rho) \cdot \exp(-B t/2) \cdot (1-t/t_0)/4\pi, \quad (2)$$

Here k is the c.m. momentum of \bar{p} , B is the slope parameter, $t = 2k^2(1 - \cos \theta)$ is the square momentum transfer, σ_{tot} is the total $\bar{p}{}^4\text{He}$ scattering cross section, $\rho = \text{Re} F_{\text{nucl}}(0)/\text{Im} F_{\text{nucl}}(0)$, t_0 is a complex parameter, corresponding to the zero of the scattering amplitude. The $\text{Re}(t_0)$ is determined by the position of the minimum in $d\sigma/d\Omega$, while $\text{Im}(t_0)$ is related to the value of $d\sigma/d\Omega$ at the minimum.

Table 2. $d\sigma/d\Omega$ at $P=192.8$ MeV/c

$d\sigma/d\Omega$ mb/sr	\pm	σ mb/sr	$\theta_{\text{c.m.}}$ deg.	bin deg.
124.94		15.15	14.2	5
92.49		10.21	19.5	5
74.69		8.20	24.5	5
74.89		7.27	29.3	5
65.25		6.22	34.5	5
51.80		5.23	39.5	5
51.23		4.95	44.6	5
35.86		3.98	49.4	5
34.25		3.74	54.6	5
16.63		2.54	59.3	5
13.30		2.22	64.2	5
9.28		1.82	68.7	5
4.14		1.19	74.7	5
2.01		0.58	82.3	10
1.17		0.44	94.1	10
0.52		0.30	105.6	10
0.36		0.25	111.5	10
1.19		0.49	122.8	10
1.58		0.60	132.3	10
0.87		0.50	144.8	10
1.10		0.63	153.0	10

The Coulomb amplitude $F_{\text{Coul}}(\theta)$ was evaluated taking into account the finite dimensions of the ${}^4\text{He}$ nucleus and of the antiproton applying the method described in [18].

To determine the parameters of the amplitude $F_{\text{nucl}}(\theta)$ such as σ_{tot} , ρ and B one should take into account that they are strongly correlated. To reduce the correlations we try to fix some of them from an additional experimental information. For that purpose we fit the differential cross section in the whole angular range of our measurements, determine the parameters of $F_{\text{nucl}}(\theta)$ from this fit and calculate with them the total cross section for the elastic scattering. The quality of the fit is put in evidence in Fig.2, it turns out that $\kappa^2/\text{NDF} = 1.5$. The total elastic cross section is :

$$\sigma_{\text{el}} = \int |F_{\text{nucl}}(\theta)|^2 d\Omega = 206.3 \pm 6.6 \text{ mb.} \quad (3)$$

From this value one can obtain the total $\bar{p}^4\text{He}$ interaction cross section:

$$\sigma_{\text{tot}} = \sigma_a + \sigma_{\text{el}} = 583.9 \pm 10.4 \text{ mb,} \quad (4)$$

where $\sigma_a = 377.6 \pm 8 \text{ mb}$, as obtained in this work.

For better determination of the ρ and B parameters that depend on the F_{nucl} behavior in the forward direction we fixed in (2) the value of σ_{tot} from (4) and fitted $d\sigma/d\Omega$ only for a small scattering angles region ($\theta \leq 50^\circ$) by (2), but without the factor $(1-t/t_0)$. The following results were obtained :

$$\rho = -0.17^{+0.24}_{-0.33}$$

$$B = 83.1 \pm 4.1 \text{ (Gev/c)}^{-2}. \quad (5)$$

The analysis of our elastic scattering data at 600 MeV/c [6] yielded the value $\rho = 0.22 \pm 0.05$ and $B = 58.7 \pm 1.4 \text{ (GeV/c)}^{-2}$. At 200 MeV/c the errors in the parameter ρ are quite large because the $d\sigma/d\Omega$ was measured starting from $\theta > 12^\circ$ where the sensitivity to the variation of ρ is not too strong. Nevertheless it seems that we may conclude that the ρ has negative sign at this region. It may be a reflection of the behavior of ρ in the $\bar{p}p$ elastic amplitude. It is known [19-21] that near the threshold the parameter ρ varies very rapidly with energy. Whereas from \bar{p} -atomic data it follows that ρ is large and negative $\rho = -1.08 \pm 0.09$ [21], the data at 200 MeV/c [19,20] reveal that ρ is close to zero. Owing to the Fermi smearing of the nucleon bound in ^4He

one may also expect the ρ parameter in $\bar{p}^4\text{He}$ scattering tends to be negative. However, a detailed analysis taking into account the $\bar{p}n$ interaction is needed.

Knowledge of the parameters of the amplitude $F_{\text{nucl}}(\theta)$ in (2) allows to perform partial wave projection and to determine partial wave amplitudes T_L .

$$T_L = k \frac{2L+1}{2} \int F_{\text{nucl}}(\theta) P_L(\cos\theta) d(\cos\theta), \quad (5)$$

where $P_L(\cos\theta)$ are Legendre polynomials.

The fit for determining $F_{\text{nucl}}(\theta)$ was performed for the entire angular interval with σ_{tot} from (4). One may obtain two sets of T_L which differ by the sign of $\text{Im}(t_0)$. Both sets give the same $d\sigma/d\Omega$ and χ^2 in the fitting procedure. The values of T_L are given in Table 3.

Table 3. Partial amplitudes T_L from (5)

L	I set ($\text{Im } t_0 > 0$)		II set ($\text{Im } t_0 < 0$)	
	Re T_L	Im T_L	Re T_L	Im T_L
0	-0.325	0.465	-0.045	0.537
1	-0.221	0.395	-0.233	0.387
2	-0.073	0.145	-0.099	0.129
3	-0.016	0.032	-0.024	0.027

From inspection of Table 3 one may conclude that in order to reproduce the $d\sigma/d\Omega$ at 200 MeV/c it is necessary to take into account only S, P and D partial waves. This differs from the situation at 600 MeV/c where the partial waves up to $L=7$ contribute to $d\sigma/d\Omega$.

In Fig.2 comparison with the "fuzzy black disk" model, i.e. a black disk with a diffuse boundary [22] is performed. This model proved rather successful in the phenomenological analysis of antiproton elastic scattering on different nuclei [7]. In this model the effect of surface diffuseness is taken into account by the function:

$$D(\theta) = \exp(-\Delta^2 k^2 \sin^2\theta/2) \quad (6)$$

and the scattering cross section is given by

$$d\sigma/d\Omega = (kR^2)^2 J_1^2(x)/x^2 D(\theta)^2. \quad (7)$$

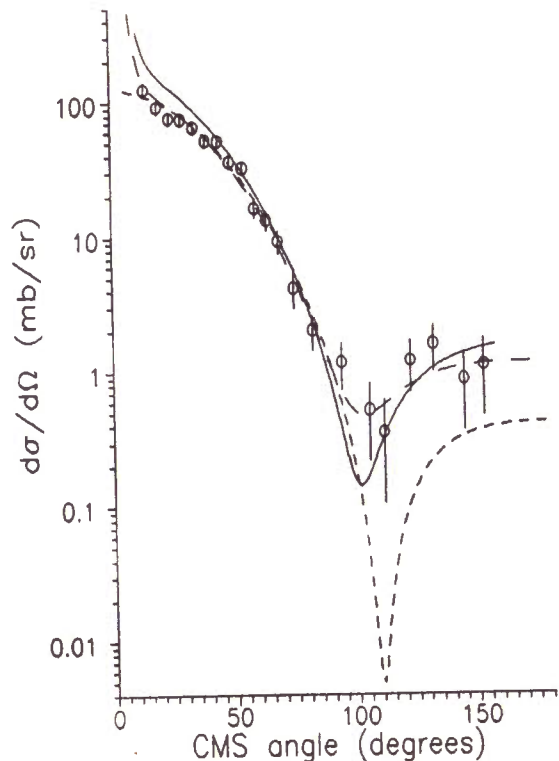


Fig.2. Differential $\bar{p}^4\text{He}$ elastic cross section at $P=192.8$ MeV/c. Solid curve -Glauber model calculation. Dashed lines - black disk fit (short dashes) and best fit by formula (1) (long dashes).

The dashed line in Fig.2 corresponds to a fuzzy black disk model fit with $R = 3.04 \pm 0.03$ fm and $\Lambda = 1.17 \pm 0.07$ fm. Performing this fit we have averaged the calculated cross sections over bins of the angular distribution. One can see that this model is good in the forward direction but cannot reproduce the $d\sigma/d\Omega$ around the minimum and at large angles. The value of the diffuseness parameter Λ turned out to be the same as for other nuclei (where $\Lambda \approx 1$ fm) [7]. This is a consequence of the large effective radius of \bar{p}^A interaction.

In Fig.2 comparison between experimental data and the predictions of the Glauber model (solid line) is performed. The calculations have been made as described in [14,23]. One can see that the Glauber model prediction overestimates the $d\sigma/d\Omega$ in the forward direction by the factor 1.5-2 and shifts the position of

the minimum in $d\sigma/d\Omega$ on $10-15^\circ$. However, at such low energy the very applicability of the Glauber model is strongly questionable.

In conclusion, the antiproton ^4He interaction at 192.8 MeV/c is investigated. Charged prong multiplicities in $\bar{p}^4\text{He}$ annihilation and the differential elastic cross section are measured. The antiproton ^4He annihilation cross section is found to be $\sigma_a = 377.6 \pm 8.0$ mb. The elastic cross section $\sigma_{el} = 206.3 \pm 6.6$ mb and the total $\bar{p}^4\text{He}$ cross section $\sigma_{tot} = 583.9 \pm 10.4$ mb are obtained.

From the fit of the differential elastic cross section the ratio of the real to imaginary part of the forward antiproton - nucleus amplitude is found: $\rho = -0.17^{+0.24}_{-0.33}$.

Partial wave decomposition of the antiproton nucleus amplitude reveals that S, P and D-waves are essential at this energy.

The fuzzy-black-disk model and Glauber model calculations do not provide the same good description of the $\bar{p}^4\text{He}$ elastic scattering at 200 MeV/c, as the one obtained at 600 MeV/c.

References

1. R. Bizzarri et al., Nuov.Cim.A 22 (1974) 225 .
2. G.Brüge et al., Phys.Rev.C 37 (1988) 1345 .
3. D.Garreta et al., Phys.Lett.B 135 (1984) 266.
4. D.Garreta et al., Phys.Lett.B 149 (1984) 64 .
5. G.Brüge et al., Phys.Lett.B 169 (1986) 14 .
6. Yu.A.Batusov et al., Sov.J.Nucl.Phys. 52 (1990) 1222.
7. J.Lichtenstadt et al., Phys.Rev.C 32 (1985) 1096.
8. I.V.Falomkin et al., Nucl. Instr. and Meth. 53 (1967) 226.
9. F.Balestra et al., Nucl.Instr. and Meth. 234 (1985) 30 .
10. R.K.Böck and J.Zoll, Report CERN/D.Ph. 2/Progr. 74-4.
11. F.Balestra et al., Nucl.Instr. and Meth.A 257 (1987) 114.
12. F.Balestra et al., Phys.Lett.B 165 (1985) 265.
13. F.Balestra et al., Nuov.Cim.A 100 (1988) 323.
14. F.Balestra et al., in proc. of First biennial conference on "Low Energy Antiproton Physics", World Scientific, Singapore, (1991) 245;
15. G.Bendisoli, Report FNT/BE-91/34, Pavia (1991) .
16. Chechetkin V.M. et al., Phys.Lett., B118 (1982) 329 .
17. Batusov Yu.A. et al., JINR Rapid Comm., n6 (1985) 11; Lett.Nuov.Cim. 41 (1984) 223.
18. K.M.Das B.B.Deo Phys.Rev.C 26 (1982) 211.
19. W.Brückner et al., Phys.Lett.B158 (1985) 180.
20. L.Linsen et al., Nucl.Phys.A 469 (1987) 726.
21. C.J.Batty Rep.Prog.Phys. 52 (1989) 1165.
22. E.V.Inopin, Berezhnoy Yu.A., Nucl.Phys., 63 (1965) 689.
23. G.Bendisoli et al., Report FNT/BE-9/03, Pavia (1991) .

Received by Publishing Department
on July 1, 1992.